

Article

Boosting the Catalytic Performance of Au-Pd/Graphene Oxide Nanocomposites via the Controlled Oxidation of Graphene Sheets

Abdullah S. Alshammari *, Alaa Abd Alfatah and Muhammad M. Alabdi

Department of Physics, College of Science, University of Hail, Hail P.O. Box 2440, Saudi Arabia

* Correspondence: ashammari@uoh.edu.sa

Abstract: Nanocomposite materials have demonstrated excellent performance in many application fields. Metal nanoparticle/graphene oxide composites are among the most promising composite materials for catalytic applications. In this study, nanocomposites of Au-Pd bimetallic particles/graphene oxide were prepared from an aqueous bath and used as catalysts in the oxidation reactions of some chemical compounds. The oxidation and exfoliation of graphite were controlled by varying the acid treatment time. The effects of the treatment time on the properties and performance of the prepared bimetallic-nanoparticle-supported graphene oxide catalysts were very obvious. Depending on the treatment time, a significant improvement in the conversion efficiency ranging from 65% to about 480%, along with a high oxidation selectivity, were achieved. The obtained findings show that the catalytic performance of metal/graphene oxide nanocomposites can be easily maximized by controlling the oxidation and exfoliation of graphene sheets.

Keywords: graphene oxide; Au-Pd nanoparticles; nanocomposites; catalytic performance



Citation: Alshammari, A.S.; Abd Alfatah, A.; Alabdi, M.M. Boosting the Catalytic Performance of Au-Pd/Graphene Oxide Nanocomposites via the Controlled Oxidation of Graphene Sheets. *J. Compos. Sci.* **2024**, *8*, 82. <https://doi.org/10.3390/jcs8030082>

Academic Editor: Francesco Tornabene

Received: 30 December 2023

Revised: 12 February 2024

Accepted: 19 February 2024

Published: 23 February 2024



Copyright: © 2024 by the authors. Licensee MDPI, Basel, Switzerland. This article is an open access article distributed under the terms and conditions of the Creative Commons Attribution (CC BY) license (<https://creativecommons.org/licenses/by/4.0/>).

1. Introduction

Nanocomposites of graphene oxide and metal nanoparticles are among the functional materials that have led to an important advancement in many application fields, including energy, sensors and catalysts [1,2]. In comparison to transition-metal-based catalysts, noble metal catalysts usually show improved catalytic activity [3]. Bimetallic nanoparticles in particular have been shown to be highly desirable materials for catalytic applications due to their excellent physical and chemical properties [2]. The electronic and energetic properties of bimetallic nanoparticles have been intensively investigated in various theoretical studies. These studies have revealed that core-shell bimetallic structures generally show improved catalytic properties, especially when they attached to a suitable support material such as graphene or graphene oxide (GO) [4]. The improved catalytic activity of such system is attributed to the interaction between the metallic structures and the graphene, which modulates the Fermi level of these materials and results in a maximized catalytic performance [5,6]. In this context, considerable interest has been devoted to graphene-supported Au-Pd bimetallic nanoparticle composites. Supported Pd catalysts exhibit a high catalytic activity that can be controlled by adjusting the particle size and their interaction with the support material [3]. Au nanoparticles also have interesting plasmonic properties for photocatalytic applications in addition to their enhanced catalytic performance when they are combined with other noble metals [7]. Combining Au and Pd produces bio-compatible, electrochemically stable and electrically conductive bimetallic nanoparticles that can be used in various catalytic applications, including fuel cells, hydrogen production, hydrogenation and alcohol oxidation [5,8–10]. On the other hand, graphene and its derivatives are considered highly suitable supports for Au-Pd-nanoparticle-based catalysts [5]. Graphene exhibits a large surface area, high electrical conductivity, high thermal conductivity, good chemical stability and high mechanical strength [5,9]. The large surface area of graphene

provides an appropriate platform to immobilize bimetallic nanoparticles with good control over their shape, size and size distribution [5]. Additionally, changing the sp^2 -to- sp^3 hybridization ratio as a result of graphene functionalization processes allows the tuning of its physical properties and its performance in many catalytic applications. The presence of functional groups also facilitates successful attachment of the metallic particles to the functionalized graphene surface [11]. The use of Au-Pd bimetallic nanoparticles along with graphene-based supports for catalytic applications has been addressed in many studies. A study by Zhang et al. investigated the oxidation of benzyl alcohol into benzaldehyde using Au-, Pd- and Au-Pd/reduced graphene oxide (rGO) composites and showed that the bimetallic-based composite exhibits the highest performance. The study attributed the improved performance of the bimetallic-based composite mainly to the small particle size [12]. It has also been shown that metallic nanoparticles are the main active elements in the oxidation process of benzyl alcohol [12]. Similarly, Chen et al. have reported that a nanocomposite of Au-Pd/GO shows a better peroxidase activity than that of Au/GO and Pd/GO composites. According to the study, the obtained superior catalytic performance in 3,3,5,5-tetramethylbenzidine (TMB) oxidation is due to the unique core-shell structure of the bimetallic nanoparticles, which allows for the maximum electronic interactions between the two metals and maximizes the contact of Pd, the shell, with the reactants [13]. Bawaked and co-workers have reported that the Au:Pd molar ratio in a graphite-supported Au-Pd bimetallic catalyst also plays a major role in determining the catalytic activity of the catalyst toward cis-cyclooctene conversion [14]. They achieved the best catalytic activity with a Au/Pd molar ratio of 0.35/0.65 in the nanocomposite. Furthermore, according to their study, the selectivity of cyclooctene oxidation into epoxide, alcohol, ketone and hydroperoxide remained unaffected by variations in the Au/Pd molar ratio [14]. The preparation of a Au-Pd/GO nanocomposite with a high catalytic performance for the reduction of 4-nitrophenol into 4-aminophenol has been reported by He et al. [15]. The authors in that study developed a simple method for preparing spherical and flower-like bimetallic nanoparticles on GO without utilizing reducing agents or surfactants. They also found that the nanocomposite with the flower-like nanoparticles exhibits a higher catalytic activity than that with spherical nanoparticles [15]. Li et al. have also developed a green wet chemical method to synthesize rGO-supported worm-like Au-Pd nanostructure composites and utilized the prepared composites for nitrite detection. The prepared nanocomposites showed a linear response over a wide concentration range with a fast response and a high detection sensitivity. The study attributed the improved detection performance of the prepared Au-Pd/rGO nanocomposite to the high surface-to-volume ratio as well as the enhanced electrical conductivity of the rGO and bimetallic nanostructures [16]. Moreover, the direct synthesis of a nano-alloyed Au-Pd/graphene composite without using stabilizing molecules and with an enhanced photocatalytic performance has been reported by Zhang et al. [17]. The study has shown that the prepared composite exhibits a high photocatalytic activity in degrading Rhodamine B under visible light irradiation and attributed the improved photocatalytic performance to the improved lifetime and efficient transfer of the charge carriers [17]. Yu et al. have investigated the effect of the carbonaceous support type on the performance of Au/rGO, Au/activated carbon and Au/graphite composites in the aerobic oxidation of benzyl alcohol [18]. They have found that the catalytic performance of the prepared nanocomposites strongly depends on the support type, with the Au/rGO composite showing the highest catalytic activity. Based on the study, the improved performance of the Au/rGO composite is attributed to the presence of surface oxygen functional groups [18]. These studies and many others on graphene-supported Au-Pd bimetallic catalysts have focused on investigating the effect of various parameters, including the particle size; particle shape; Au/Pd ratio; catalyst preparation methods, including various proposed green synthesis routes; the attachment methods of the bimetallic particles to the support surface and the type of the carbonaceous support on the catalysts' performance [1,4-6,9,12-18]. Yet, the influence of the preparation methods and treatment conditions of graphene and its derivatives as support materials on the catalytic activity

of graphene/Au-Pd bimetallic nanoparticles has rarely been investigated and requires intensive exploration. Therefore, the current work reports an investigation of the effect of the graphene's oxidation treatment time on its catalytic activity with the attached bimetallic nanoparticles. The prepared graphene oxide/Au-Pd NPs catalysts were tested for the conversion of benzylic alcohols into some fine chemicals. The oxidation of benzylic alcohols into benzaldehyde is of great importance in many food-related, cosmetics, perfume and pharmaceutical industrial processes [12].

2. Materials and Methods

The Au-Pd particles/graphene oxide nanocomposites were prepared using a simple chemical route and were characterized using different techniques. To prepare the GO, the procedures used in our previous study on CNTs were followed [19,20]. Briefly, 10 mL of nitric acid was mixed with 30 mL of sulfuric acid, and then 200 mg of raw graphite powder was added to the mixture. The mixture was then heated to 75 °C and was kept under continuous stirring (@ 300 rpm) for different times, from 30 min to 120 min. After the acid treatment time was completed, the mixture was left to cool down to room temperature and was then filtered and washed with DI water several times until a PH value of 7 was achieved. After that, the samples were left in a drying oven at 110 °C overnight to remove the water. The Au-Pd bimetallic nanoparticles were grown on the GO by adding an aqueous solution of HAuCl₄ (12.25 mg/mL) and then PdCl₂ (6 mg/mL) to 1000 mL of distilled water with continuous stirring. Then, 0.65 mL of polyvinyl alcohol aqueous solution (10 mg/mL) was added as a stabilizing ligand. After 15 min, 0.82 mL of a 0.2 M NaBH₄ fresh aqueous solution was added as a reducing agent under stirring for 30 min. Then, the GO support (0.495 g) was introduced into the mixture, along with a few drops of concentrated sulfuric acid (H₂SO₄), and left under stirring for another hour. The resulting catalyst was recovered using filtration and was then dried for 24 h at 110 °C. The Au/GO and Pd/GO nanocomposites (with the GO treated for 60 min) were also prepared using the same procedures described above, and their catalytic performance was evaluated and compared with that of the Au-Pd/GO nanocomposite samples. To test the catalytic performance of the nanocomposite samples, 20 mg of the nanocomposite catalysts was added to 2 mL of benzyl alcohol in a reactor under oxygen pressure of 1 bar, 1000 rpm cycles and 120 °C for 2 h. After completing the reaction, the samples were left to cool down to room temperature and were then centrifuged to recover the catalyst. Finally, a sample from each catalyst vial was withdrawn and examined using the Varian CP-3800 gas chromatograph (GC). Table 1 summarizes the samples used in this study and their preparation conditions.

Table 1. The prepared Au-Pd/GO nanocomposite samples.

Sample	Structure	Graphite Treatment	Treatment Time
G 0	Au-Pd/Graphite	No	-
G 1	Au-Pd/GO	Yes	30 min
G 2	Au-Pd/GO	Yes	60 min
G 3	Au-Pd/GO	Yes	90 min
G 4	Au-Pd/GO	Yes	120 min

3. Results

The prepared GO-supported Au-Pd bimetallic nanoparticle composites were investigated using various techniques. Figure 1 shows SEM images of the graphite sample before (Figure 1a) and after (Figure 1b,c) the exfoliation of the GO layers. It can be seen from the figure that after the chemical treatment and exfoliation of the three-dimensional graphite structure, a few layers graphene oxide is produced. No obvious presence of the grown Au-Pd bimetallic nanoparticles on the surface of the exfoliated GO layers was observed in the SEM images due to their small size. However, EDS analysis of the prepared samples

confirmed the presence of the elements Au and Pd, as shown in Figure 2, which indicates the formation of the bimetallic nanoparticles on the support material.

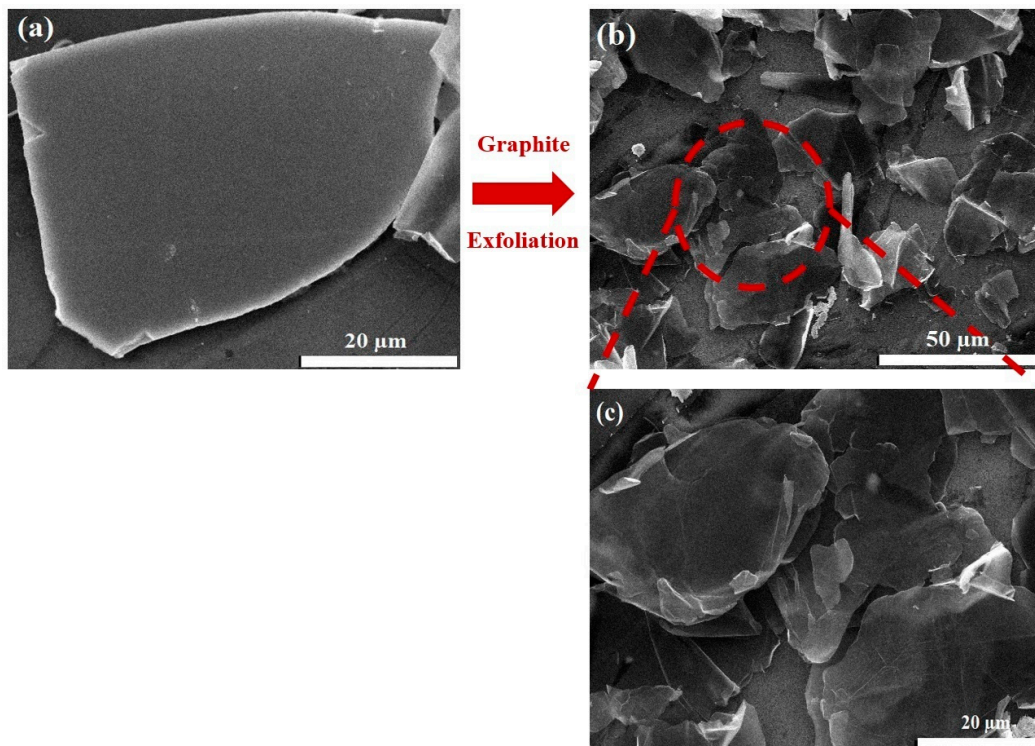


Figure 1. (a) SEM image of graphite, (b) SEM image of GO after chemical exfoliation and (c) magnified SEM image of GO after exfoliation.

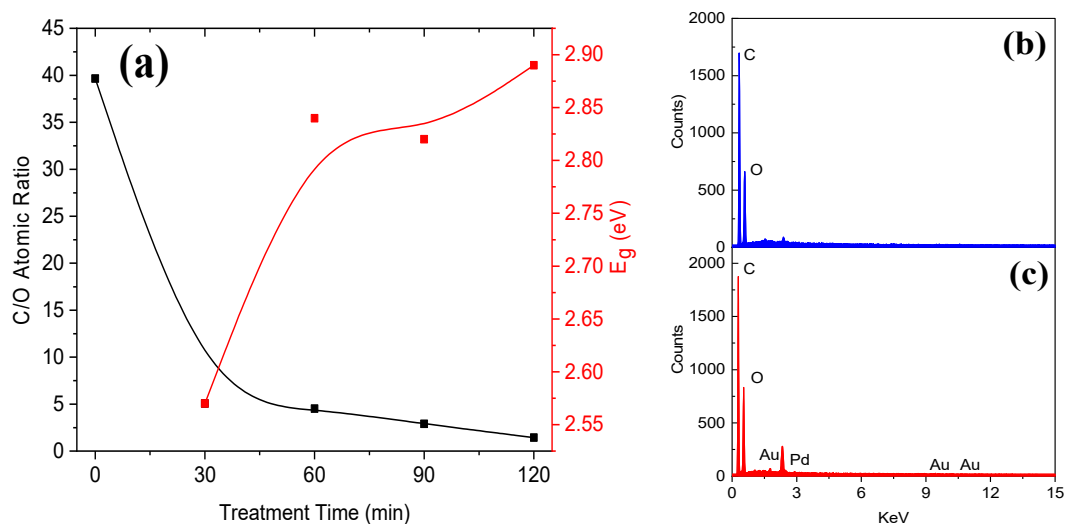


Figure 2. (a) EDS analysis and band gap variation in GO samples treated at different times, (b) EDS spectrum of GO sample and (c) EDS spectrum of Au-Pd-supported GO nanocomposite.

The effect of the GO treatment time on the composition of the prepared sample was investigated by collecting the EDS spectra of the samples. Figure 2a shows the variation in the carbon-to-oxygen ratio in the GO samples as a function of the treatment time. It can be seen from the figure that the C/O ratio in the case of the untreated sample (graphite sample) is about 40 and decreases as the treatment time increases to about 1.44 for the sample oxidized for 120 min. The decrease in the C/O ratio is mainly due to the increase in the

oxygen content in the sample as a result of the oxygen functional groups' attachment to the graphene layers. The results indicate that the density of these functional groups increases with the treatment time. The figure also shows the variation in the band gap of the produced GO layer with the different used treatment times. The relation $(\alpha hv) = A (hv - E_g)^n$ was used to calculate the band gap of the GO layers where α is the absorption coefficient, hv is the incident photons' energy, A is a constant, E_g is the band gap of the GO layers and n is a parameter that has the values $\frac{1}{2}$ and 2 for direct and indirect transitions, respectively [21]. It can be seen from the figure that the band gap values of the GO samples increase with the treatment time. The increase in the band gap when increasing the treatment time can be attributed to the introduced oxygen functional groups. An increase in the band gap upon graphene oxidation has been reported in various studies [22].

Figure 2b,c show a comparison of the EDS spectra of the GO before and after the growth of the Au-Pd nanoparticles. The top spectrum (2b) shows the presence of carbon and oxygen in the oxidized graphene sample and confirms the presence of oxygen functional groups in the sample. The EDS spectrum at the bottom (2c) shows an elemental analysis of the nanocomposite sample and confirms the growth of the Au-Pd nanoparticles as the Au and Pd elements are present in the sample in addition to the C and O of the GO layers. The atomic ratio of Au to Pd (Au/Pd) was found from the EDS analysis to be about 3.75 in the nanocomposite samples.

Figure 3 shows the TEM studies of the prepared nanocomposite samples. Figure 3a shows the exfoliated GO sheet with a few-layers structure. In Figure 3b, a magnified image of a GO sheet is shown, where it directly confirms the successful growth of Au-Pd bimetallic nanoparticles on the oxidized graphene sheets. The immobilization of Au-Pd nanoparticles onto graphene sheets has been shown to occur through covalent bonding in various studies [9,23,24]. Moreover, Figure 3b shows that the grown spherical nanoparticles are of different sizes and are uniformly distributed over the GO sheets. The magnified image in the inset of Figure 3b does not show any presence of core-shell or hetero-structure growth of the bimetallic nanoparticles, which suggests the formation of alloyed nanoparticles. The size distribution of the bimetallic nanoparticles is shown in Figure 3c. The grown nanoparticles exhibit a narrow size distribution, as seen from the figure, with an average size of 3.18 ± 0.05 nm. The small nanoparticle size with a high surface area is expected to significantly contribute to the catalytic performance of the prepared nanocomposites.

Figure 4a illustrates the XRD patterns of the prepared nanocomposite samples. The peak at 2θ of about 25.8° is the (002) diffraction peak of the GO [25]. The intensity of the peak is high for the sample treated for 30 min and decreases as the treatment time is increased to 60, 90 and 120 min, along with an obvious broadening of the peak, which indicates the clear effect of the treatment time on the structural properties of the GO sheets. Moreover, a slight shift in the peak position toward low 2θ values is seen from the figure with an increasing treatment time. This shift in the (002) peak position indicates an increase in the interplanar distance, which can be attributed to the incorporation of the oxygen functional groups on and between the GO layers [26]. The interplanar distance for the treated GO samples was estimated from the XRD patterns using the relation $n\lambda = 2d\sin\theta$, where n is the reflection order, λ is the X-ray wavelength, d is the interplanar distance and θ is the X-ray diffraction angle [27]. The interplanar distance values were found in the range of 0.351 to 0.354 with an increasing acid treatment time. These values are higher than the interplanar distance of graphite (0.34 nm), indicating the successful insertion of oxygen functionalities between the GO layers [28]. Another low-intensity peak can be observed in the figure at $2\theta \approx 44^\circ$, which is the diffraction peak of the (200) plane of Au. The diffraction peak at $2\theta \approx 72.8^\circ$ at a position between the (220) plane of Pd (JCPDS#05-0681) and the (311) plane of Au (JCPDS#04-0784) may indicate the formation of alloyed Au-Pd nanoparticles, which supports the observations from the TEM images of the grown nanoparticles [12]. The increase in the intensity of this peak with an increasing GO treatment time also indicates the improvement in the crystallinity of the grown bimetallic nanoparticles and their density in the prepared samples. The last peak at about 87° is the diffraction peak from the Pd's

(222) atomic plane [12]. The presence of these peaks confirms the successful formation of the Au-Pd nanoparticles on the GO surface as alloyed nanoparticles, with probably a greater Au content at the core and a greater Pd ratio at the particle surface.

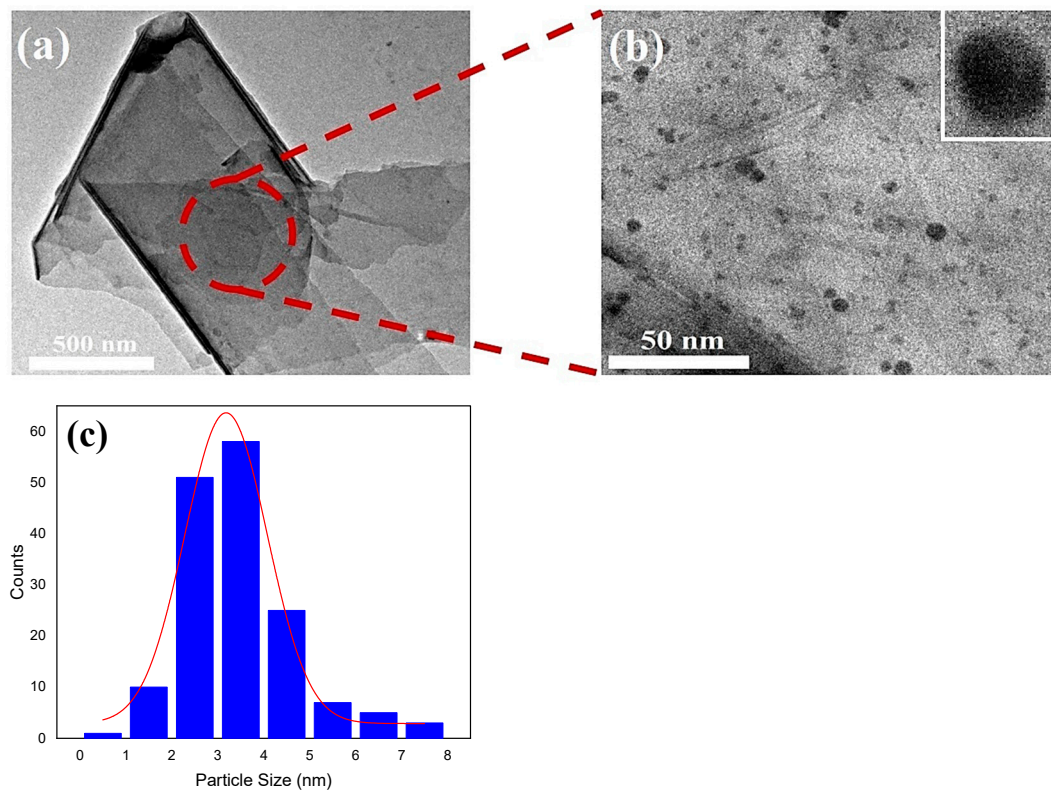


Figure 3. (a) TEM image of exfoliated graphene oxide, (b) a magnified TEM image of graphene oxide showing the successful growth of uniformly distributed Au-Pd bimetallic nanoparticles with the inset showing a magnified image of a single nanoparticle and (c) a histogram distribution of Au-Pd bimetallic nanoparticle size with a mean value of 3.18 ± 0.05 nm.

The effect of the acid treatment on the prepared sample is also shown in Figure 4b. A clear variation in the diffraction peak of the GO can be seen clearly from the figure. As the treatment time increases, the peak FWHM increases. This increase in the peak FWHM is an indication of the GO's crystallinity deterioration, which results from converting the crystalline sp^2 carbon hybridization into amorphous sp^3 carbon hybridization after the introduction of the oxygen functionalities onto the graphene surface [29,30].

Figure 4c shows the FTIR spectra of the prepared nanocomposite samples with the presence of many absorption bands. The peak at about 3500 is the specific peak of O-H stretching, which mainly results from the attachment of the hydroxyl groups to the graphene's surface [6]. Other absorption bands corresponding to C-H, C=O, C=C and C-O stretching can also be seen at 2921, 1750, 1648 and 1070, respectively. The absorption band appearing at about 1210 cm^{-1} is attributed to the epoxy C-O-C bending and that at about 1324 cm^{-1} is the carboxyl C-OH bending vibration [11,12,31]. It is also interesting to note that the intensity of the stretching O-H band is slightly reduced after the nanoparticles' growth and with an increasing treatment time, which could be linked to the grown particles' density in the samples. The oxygen-containing functionalities can assist with the trapping of Au and Pd ions and hence the formation of bimetallic nanoparticles, along with diminishing the absorption intensities of these functionalities [2,8,9]. This effect can also be seen from the comparison given in Figure 4d between the FTIR spectrum of the GO sample and that of the sample after the attachment of the Au-Pd nanoparticles. It is also seen from the figure that the absorption band intensity of the oxygen functionalities is reduced after the formation of the composite.

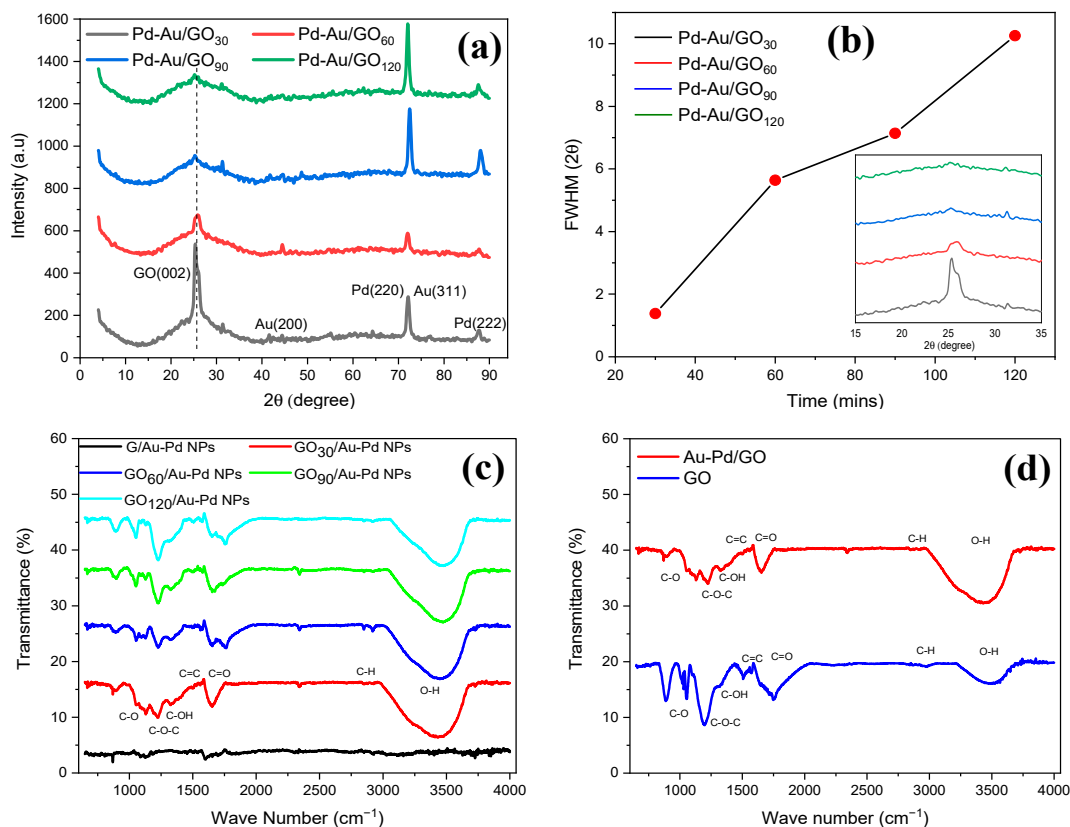


Figure 4. (a) XRD patterns of the GO/Au-Pd bimetallic particle nanocomposites, (b) widening of the FWHM of the GO peak with the different treatment conditions, (c) FTIR spectra of the GO/Au-Pd bimetallic particle nanocomposites and (d) FTIR spectra of the GO layers and GO/Au-Pd bimetallic particle nanocomposites.

The catalytic performance of the Au-Pd/GO nanocomposite samples was tested for converting benzyl alcohol into benzaldehyde, which is considered to be among the most important reactions in many industrial processes. The reaction mechanism of benzyl alcohol's conversion into fine chemicals using a Au-Pd/graphene catalyst has been reported in various previous studies [32,33]. Figure 5 shows the performance evaluation results of the prepared nanocomposite samples. The selectivity toward converting benzyl alcohol into benzaldehyde is shown in Figure 5a. All the samples show a high selectivity in the oxidation of benzyl alcohol into benzaldehyde of more than 95%. The Au-Pd/graphite sample shows the highest selectivity (~99.8%) while the GO-supported samples exhibit a selectivity in the range of 95–96.3%. The samples also show low selectivity in the oxidation of benzyl alcohol into toluene in the range of 3.7–5.0%.

In addition to the evaluation of the selectivity of the nanocomposite samples, the conversion performance of the Au-Pd/GO nanocomposite samples was also evaluated in comparison with the Au-Pd/graphite nanocomposite sample. The performance comparison was obtained using the equation $\frac{\Delta P}{P} \% = \left| \frac{P_{Au:Pd/G} - P_{Au:Pd/GO}}{P_{Au:Pd/G}} \right| \times 100$. Figure 5b shows the comparison results of the different prepared samples with the graphite-supported nanoparticle sample. It is seen from the figure that as the treatment time of the graphite increases, the catalytic performance of the samples significantly increases and reaches a high value of about 480% for the bimetallic nanoparticle sample supported on the 120 min treated GO. This improvement in the catalytic performance of the treated samples can be attributed to the presence of the functional groups on the graphene surface after the acid treatment. Increasing the treatment time breaks the C-C bonds and introduces oxygen functionalities with a high density. These functional groups serve as nucleation centers that facilitate the growth/attachment of the Au-Pd bimetallic nanoparticles [2,34]. Therefore,

the samples treated for a longer time are expected to have, due to the effective exfoliation of the graphene layer, a high nanoparticle density and hence the observed enhancement in the catalytic performance. Moreover, to further investigate the catalytic performance of the prepared samples, the performance of the GO nano-sheets, Au/GO nanocomposite and Pd/GO nanocomposite was evaluated and compared with that of the Au-Pd/GO nanocomposite for the GO sample treated for 60 min, as shown in Figure 5b. As seen from the figure, the Au-Pd/GO sample showed the highest performance, followed by Au/GO, Pd/GO and finally the GO sample, which exhibited the lowest performance. The improved performance of the bimetallic sample was expected, as similar observations have been reported elsewhere [12]. However, the achieved performance enhancement via controlling the oxidation of GO, the support material, highlights the significance of the findings of the current study. These findings show the importance of the acid treatment conditions and the possibility of utilizing their parameters to significantly boost the catalytic activity of the graphene-based nanocomposite catalysts.

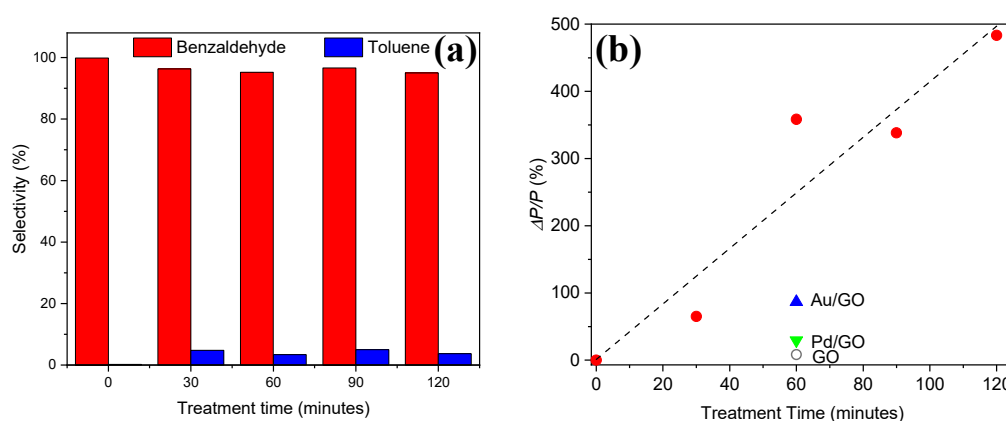


Figure 5. The performance of the prepared nanocomposite samples in benzyl alcohol oxidation: (a) selectivity of Au-Pd/GO nanocomposite samples with different GO treatment times and (b) catalytic performance enhancement of Au-Pd/GO nanocomposite samples with different GO treatment times (red solid spheres).

4. Conclusions

Nanocomposites of Au-Pd bimetallic particles/graphene oxide were successfully prepared and utilized as catalysts in the oxidation reactions of some chemicals. The acid treatment time was utilized to control the oxidation level and exfoliation of the graphite. The EDS analysis revealed a decrease in the C/O ratio when increasing the treatment time, which indicates an increase in the oxygen content in the treated samples. The increase in the oxygen content was also found to be accompanied by an increase in the band gap of the treated GO samples. Microscopic studies showed highly exfoliated graphene layers with a uniform growth of Au-Pd bimetallic nanoparticles in the size range of a few nanometers. XRD studies also confirmed the growth of the nanoparticles and showed a clear crystallinity disturbance in the graphene layers as a result of the increased acid treatment time. The evaluation of the catalytic performance of the prepared bimetallic-nanoparticle-supported graphene oxide showed a significant improvement in the conversion performance of up to 480% in comparison with the untreated-graphite-supported samples and with a high conversion selectivity of benzyl alcohol into benzaldehyde. The improved catalytic performance with an increasing GO treatment time is attributed to the enhanced dispersion of the GO sheets and the increased density of the attached bimetallic nanoparticles. Additionally, the catalytic performance of both the Au/GO and Pd/GO nanocomposites and that of GO nano-sheets was evaluated and was found to be lower than that of the bimetallic Au-Pd/GO nanocomposites. The results showed that the acid treatment time used to oxidize graphene is a key factor in improving its properties as a supporting material for

Au-Pd bimetallic nanoparticles and for improving their catalytic performance. Exploring the effect of a wider treatment time range and different treatment temperatures on the nanocomposites' catalytic properties and the related catalytic performance would be of great importance.

Author Contributions: A.S.A.: conceptualization, methodology, visualization, formal analysis, investigation, writing—original draft; A.A.A.: investigation, formal analysis; M.M.A.: investigation, formal analysis. All authors have read and agreed to the published version of the manuscript.

Funding: This research was funded by the deanship of scientific research at the University of Hail (project no. 0150493).

Data Availability Statement: The data presented in this study are available from the corresponding author upon reasonable request.

Acknowledgments: The authors would like to thank Hamed Alshammari and Jamal Humaidi for their help and the useful discussion.

Conflicts of Interest: The authors declare no conflicts of interest.

References

1. Zhou, H.; Chen, L.; Li, S.; Huang, S.; Sun, Y.; Chen, Y.; Wang, Z.; Liu, W.; Li, X. One-step electroreduction preparation of multilayered reduced graphene oxide/gold-palladium nano hybrid as a proficient electrocatalyst for development of sensitive hydrazine sensor. *J. Colloid Interface Sci.* **2020**, *566*, 473–484. [[CrossRef](#)] [[PubMed](#)]
2. Jahromi, M.N.; Tayadon, F.; Bagheri, H. A new electrochemical sensor based on an Au-Pd/reduced graphene oxide nanocomposite for determination of Parathion. *Int. J. Environ. Anal. Chem.* **2020**, *100*, 1101–1117. [[CrossRef](#)]
3. Bi, F.; Ma, S.; Gao, B.; Liu, B.; Huang, Y.; Qiao, R.; Zhang, X. Boosting toluene deep oxidation by tuning metal-support interaction in MOF-derived Pd@ZrO₂ catalysts: The role of interfacial interaction between Pd and ZrO₂. *Fuel* **2024**, *357*, 129833. [[CrossRef](#)]
4. Wang, B.; Chang, T.-Y.; Gong, X.; Jiang, Z.; Yang, S.; Chen, Y.-S.; Fang, T. One-pot synthesis of Au/Pd core/shell nanoparticles supported on reduced graphene oxide with enhanced dehydrogenation performance for dodecahydro-N-ethylcarbazole. *ACS Sustain. Chem. Eng.* **2018**, *7*, 1760–1768. [[CrossRef](#)]
5. Al-Nayili, A.; Albdiry, M. AuPd bimetallic nanoparticles supported on reduced graphene oxide nanosheets as catalysts for hydrogen generation from formic acid under ambient temperature. *New J. Chem.* **2021**, *45*, 10040–10048. [[CrossRef](#)]
6. Darabdhara, G.; Amin, M.A.; Mersal, G.A.; Ahmed, E.M.; Das, M.R.; Zakaria, M.B.; Malgras, V.; Alshehri, S.M.; Yamauchi, Y.; Szunerits, S.; et al. Reduced graphene oxide nanosheets decorated with Au, Pd and Au-Pd bimetallic nanoparticles as highly efficient catalysts for electrochemical hydrogen generation. *J. Mater. Chem. A* **2015**, *3*, 20254–20266. [[CrossRef](#)]
7. Lyu, X.; Liu, Q.; Yuan, Q.; Liang, X.; Chen, Q.; Luo, P.; Yang, Y.; Fang, Z.; Bao, H. Ultrafast synthesis of multi-branched Au/Ag bimetallic nanoparticles at room temperature for photothermal reduction of 4-nitrophenol. *J. Catal.* **2023**, *428*, 115174. [[CrossRef](#)]
8. Darabdhara, G.; Boruah, P.K.; Borthakur, P.; Hussain, N.; Das, M.R.; Ahamad, T.; Alshehri, S.M.; Malgras, V.; Wu, K.C.-W.; Yamauchi, Y. Reduced graphene oxide nanosheets decorated with Au-Pd bimetallic alloy nanoparticles towards efficient photocatalytic degradation of phenolic compounds in water. *Nanoscale* **2016**, *8*, 8276–8287. [[CrossRef](#)]
9. Dutta, S.; Ray, C.; Mallick, S.; Sarkar, S.; Roy, A.; Pal, T. Au@Pd core-shell nanoparticles-decorated reduced graphene oxide: A highly sensitive and selective platform for electrochemical detection of hydrazine. *RSC Adv.* **2015**, *5*, 51690–51700. [[CrossRef](#)]
10. Tadayon, F.; Vahed, S.; Bagheri, H. Au-Pd/reduced graphene oxide composite as a new sensing layer for electrochemical determination of ascorbic acid, acetaminophen and tyrosine. *Mater. Sci. Eng. C* **2016**, *68*, 805–813. [[CrossRef](#)]
11. Wang, J.; Kondrat, S.A.; Wang, Y.; Brett, G.L.; Giles, C.; Bartley, J.K.; Lu, L.; Liu, Q.; Kiely, C.J.; Hutchings, G.J. Au-Pd Nanoparticles Dispersed on Composite Titania/Graphene Oxide-Supports as a Highly Active Oxidation Catalyst. *ACS Catal.* **2015**, *5*, 3575–3587. [[CrossRef](#)]
12. Zhang, Y.; Gao, F.; Fu, M.-L. Composite of Au-Pd nanoalloys/reduced graphene oxide toward catalytic selective organic transformation to fine chemicals. *Chem. Phys. Lett.* **2018**, *691*, 61–67. [[CrossRef](#)]
13. Chen, H.; Li, Y.; Zhang, F.; Zhang, G.; Fan, X. Graphene supported Au-Pd bimetallic nanoparticles with core-shell structures and superior peroxidase-like activities. *J. Mater. Chem.* **2011**, *21*, 17658–17661. [[CrossRef](#)]
14. Bawaked, S.; He, Q.; Dummer, N.F.; Carley, A.F.; Knight, D.W.; Bethell, D.; Kiely, C.J.; Hutchings, G.J. Selective oxidation of alkenes using graphite-supported gold-palladium catalysts. *Catal. Sci. Technol.* **2011**, *1*, 747–759. [[CrossRef](#)]
15. He, Y.; Zhang, N.; Zhang, L.; Gong, Q.; Yi, M.; Wang, W.; Qiu, H.; Gao, J. Fabrication of Au-Pd nanoparticles/graphene oxide and their excellent catalytic performance. *Mater. Res. Bull.* **2014**, *51*, 397–401. [[CrossRef](#)]
16. Li, S.-S.; Hu, Y.-Y.; Wang, A.-J.; Weng, X.; Chen, J.-R.; Feng, J.-J. Simple synthesis of worm-like Au-Pd nanostructures supported on reduced graphene oxide for highly sensitive detection of nitrite. *Sens. Actuators B Chem.* **2014**, *208*, 468–474. [[CrossRef](#)]
17. Zhang, Y.; Zhang, N.; Tang, Z.-R.; Xu, Y.-J. Graphene oxide as a surfactant and support for in-situ synthesis of Au-Pd nanoalloys with improved visible light photocatalytic activity. *J. Phys. Chem. C* **2014**, *118*, 5299–5308. [[CrossRef](#)]

18. Yu, X.; Huo, Y.; Yang, J.; Chang, S.; Ma, Y.; Huang, W. Reduced graphene oxide supported Au nanoparticles as an efficient catalyst for aerobic oxidation of benzyl alcohol. *Appl. Surf. Sci.* **2013**, *280*, 450–455. [[CrossRef](#)]
19. Alshammari, A.S.; Shkunov, M.; Silva, S.R.P. Correlation between wetting properties and electrical performance of solution processed PEDOT:PSS/CNT nano-composite thin films. *Colloid Polym. Sci.* **2013**, *292*, 661–668. [[CrossRef](#)]
20. Alshammari, A.S.; Shkunov, M.; Silva, S.R.P. Inkjet printed PEDOT:PSS/MWCNT nano-composites with aligned carbon nanotubes and enhanced conductivity. *Phys. Status Solidi (RRL)-Rapid Res. Lett.* **2013**, *8*, 150–153. [[CrossRef](#)]
21. de Lima, A.H.; Tavares, C.T.; da Cunha, C.C.S.; Vicentini, N.C.; Carvalho, G.R.; Fragneaud, B.; Maciel, I.O.; Legnani, C.; Quirino, W.G.; de Oliveira, L.F.C.; et al. Origin of optical bandgap fluctuations in graphene oxide. *Eur. Phys. J. B* **2020**, *93*, 105. [[CrossRef](#)]
22. Gupta, V.; Sharma, N.; Singh, U.; Arif, M.; Singh, A. Higher oxidation level in graphene oxide. *Optik* **2017**, *143*, 115–124. [[CrossRef](#)]
23. Zhang, W.; Cheng, D.; Zhu, J. Theoretical study of CO catalytic oxidation on free and defective gra-phene-supported Au–Pd bimetallic clusters. *RSC Adv.* **2014**, *4*, 42554–42561. [[CrossRef](#)]
24. Ji, W.-X.; Zhang, C.-W.; Li, F.; Li, P.; Wang, P.-J.; Ren, M.-J.; Yuan, M. First-principles study of small Pd–Au alloy clusters on graphene. *RSC Adv.* **2014**, *4*, 55781–55789. [[CrossRef](#)]
25. Alkhouzaam, A.; Qiblawey, H.; Khraisheh, M. Polydopamine Functionalized Graphene Oxide as Membrane Nanofiller: Spectral and Structural Studies. *Membranes* **2021**, *11*, 86. [[CrossRef](#)]
26. Sardinha, A.F.; Almeida, D.A.; Ferreira, N.G. Electrochemical impedance spectroscopy correlation among graphene oxide/carbon fibers (GO/CF) composites and GO structural parameters produced at different oxidation degrees. *J. Mater. Res. Technol.* **2020**, *9*, 10841–10853. [[CrossRef](#)]
27. Oliveira, A.E.F.; Braga, G.B.; Tarley, C.R.T.; Pereira, A.C. Thermally reduced graphene oxide: Synthesis, studies and characterization. *J. Mater. Sci.* **2018**, *53*, 12005–12015. [[CrossRef](#)]
28. Yang, H.; Jiang, J.; Zhou, W.; Lai, L.; Xi, L.; Lam, Y.M.; Shen, Z.; Khezri, B.; Yu, T. Influences of graphene oxide support on the electrochemical performances of graphene oxide-MnO₂ nanocomposites. *Nanoscale Res. Lett.* **2011**, *6*, 531. [[CrossRef](#)]
29. Lee, S.-Y.; Mahajan, R.L. A facile method for coal to graphene oxide and its application to a biosensor. *Carbon* **2021**, *181*, 408–420. [[CrossRef](#)]
30. Gómez, S.; Rendtorff, N.M.; Aglietti, E.F.; Sakka, Y.; Suárez, G. Surface modification of multiwall carbon nanotubes by sulfonitic treatment. *Appl. Surf. Sci.* **2016**, *379*, 264–269. [[CrossRef](#)]
31. Bera, M.; Chandravati; Gupta, P.; Maji, P.K. Facile one-pot synthesis of graphene oxide by sonication assisted mechanochemical approach and its surface chemistry. *J. Nanosci. Nanotechnol.* **2018**, *18*, 902–912. [[CrossRef](#)] [[PubMed](#)]
32. Chan-Thaw, C.E.; Savara, A.; Villa, A. Selective Benzyl Alcohol Oxidation over Pd Catalysts. *Catalysts* **2018**, *8*, 431. [[CrossRef](#)]
33. Sharma, A.S.; Kaur, H.; Shah, D. Selective oxidation of alcohols by supported gold nanoparticles: Recent advances. *RSC Adv.* **2016**, *6*, 28688–28727. [[CrossRef](#)]
34. Alshammari, H.M.; Alshammari, A.S.; Humaidi, J.R.; Alzahrani, S.A.; Alhumaimess, M.S.; Aldosari, O.F.; Hassan, H.M.A. Au-Pd bimetallic nanocatalysts incorporated into carbon nanotubes (CNTs) for selective oxidation of alkenes and alcohol. *Processes* **2020**, *8*, 1380. [[CrossRef](#)]

Disclaimer/Publisher’s Note: The statements, opinions and data contained in all publications are solely those of the individual author(s) and contributor(s) and not of MDPI and/or the editor(s). MDPI and/or the editor(s) disclaim responsibility for any injury to people or property resulting from any ideas, methods, instructions or products referred to in the content.